Chin. J. Astron. Astrophys. Vol. 2 (2002), No. 4, 325–346
(*http://www.chjaa.org* or *http://chjaa.bao.ac.cn*)

Chinese Journal of Astronomy and Astrophysics

Multifrequency Polarization Variations in the Quasar 0917+624

Shan-Jie Qian[1,2] ⋆, A. Kraus[2], Xi-Zhen Zhang[1], T. P. Krichbaum[2], A. Witzel[2] and J. A. Zensus[2]

[1] National Astronomical Observatories, Chinese Academy of Sciences, Beijing 100012
[2] Max-Planck-Institut für Radioastronomie, Auf dem Hügel 69, 53121 Bonn, Germany

Received 2002 February 18; accepted 2002 April 20

Abstract We present a detailed analysis of multi-frequency observations of linear polarization in the intraday variable quasar 0917+624 ($z = 1.44$). The observations were made in May 1989 at five frequencies (1.4, 2.7, 5.0, 8.3 and 15 GHz) with the VLA and the Effelsberg 100 m-telescope and in December 1988 at two frequencies (2.7 and 5.0 GHz) with the latter. It is shown that the relationship between the variations of the polarized and total flux density is highly wavelength dependent, and the multi-frequency polarization behavior may be essential for investigating the mechanisms causing these variations. It is shown that the variations observed at 20 cm can be interpreted in terms of refractive interstellar scintillation. However, after subtracting the variation due to scintillation, three 'features' emerged in the light-curve of the polarized flux density, indicating an additional variable component. Interestingly, these features are shown to be correlated with the variations at 2–6 cm, thus indicating that these features and the associated variations are due to some intrinsic causes. Moreover, a very rapid polarization angle swing of $\sim 180^\circ$ observed in December 1988 which cannot be explained by refractive interstellar scintillation, may also be produced by an intrinsic mechanism. Accordingly, we use a shock model to explain the polarization variations observed at the higher frequencies, although scintillation could also exist. The shock model can explain not only the variation of intensity, but also the time variation of its degree and angle of polarization, including the rapid swing of the polarization angle. It is shown that the degree and angle of polarization of the shock need only vary slightly in order to account for the observed complicated behaviour of polarization.

Key words: radio continuum: galaxies — polarization — quasars: individual (QSO 0917+624)

⋆ E-mail: rqsj@class1.bao.ac.cn

1 INTRODUCTION

Intraday variability in compact flat-spectrum radio sources has been intensively studied since its discovery (Heeschen et al. 1987; Quirrenbach et al. 1989; Witzel 1992; Wagner & Witzel 1995). The central problem is how to explain the very high apparent brightness temperatures derived from the observed timescales, which are far in excess of the inverse-Compton limit (Kellermann & Pauliny-Toth 1969). For most of the sources observed so far, the derived apparent brightness temperature $T_{\rm b,app}$ ranges from $\sim 10^{16}$ to 10^{18} K. However, for some extreme cases the timescale of variability can be as short as ~ 1 hour, corresponding to apparent brightness temperatures $\sim 10^{21}$ K (e.g., PKS 0405–385 (Kedziora-Chudzcer et al. 1997) and J1819+385 (Dennett-Thorpe & de Bruyn 2000).

In order to understand these phenomena, both extrinsic and intrinsic mechanisms have been proposed. As the most likely extrinsic mechanism, refractive interstellar scintillation (RISS) has been suggested to explain the intraday variability, assuming that the radio sources contain very compact components with angular sizes less than $\sim 50 - 100\,\mu$as and the scattering screen lies much nearer than the 'normal' value of ~ 1 kpc (e.g., 0.2 kpc or so for 0917+624; Rickett 1990; Rickett et al. 1995; Qian 1994a, 1994b; Qian et al. 1995). For the extreme cases mentioned above, the angular size of the scintillating components was derived to be $\sim 10\,\mu$as and the distance of the screen is required to be as small as ~ 20 pc (Rickett 2002; Dennett-Thorpe & de Bruyn 2000). Nevertheless, we should point out that in these scintillation models relativistic beaming is still required to solve the apparent brightness temperature problem (Begelman et al. 1994; Coppi 1997). There seems to be a consensus that for the most extreme cases of $T_{\rm b,app} \approx 10^{21}$ K scintillation may be dominant.

However, some IDV events with $T_{\rm b,app} \sim 10^{16} - 10^{18}$ K show evidence for an intrinsic origin. For example, the correlated radio–optical intraday variations observed in the BL Lac object 0716+714 (Quirrenbach et al. 1991; Wagner et al. 1996; Qian et al. 1996) favor intrinsic mechanisms, because RISS cannot produce optical variations. In addition, some rapid polarization variations (for example, polarization angle swings of $\sim 180°$; Qian et al. 1991; Gabuzda & Kochanev 1999) may also imply intrinsic causes. Among the proposed intrinsic models, the shock models (Qian et al. 1991; Marscher 1992; Spada et al. 1999), which invoke a relativistic shock moving through the turbulence of magnetized plasma (Jones et al. 1985) or inhomogeneous structures in the jet, have been applied to explain the intraday variations in 0917+624, 0716+714 and other sources. However, even in the case of intrinsic variations, scintillation could still be present as an additional effect, because of the small size of the sources. Therefore, IDV in compact extragalactic radio sources may probably be caused by both RISS and some intrinsic mechanism. Different IDV events may imply different physical conditions (source structure, relativistic motion and interstellar medium, etc.). Recently, the VLBI observations of 0917+624 made by Krichbaum et al. (2002) at 15 GHz demonstrated that the structural changes of its core could cause the IDV timescale variations observed by Kraus et al. (1999b).

Therefore, it is very important to distinguish between variations that are intrinsic to the compact radio source and those that are primarily due to RISS, but the disentanglement of the two is very difficult, because the intraday variations are small-amplitude fluctuations. Although intensive studies of IDV in total flux density at several frequencies have been carried out in recent years (e.g., Kraus et al. 1999a; Kedziora-Chudzcer et al. 1998; Quirrenbach et al. 2000), until now none of the observed IDV events have been properly separated into intrinsic variations

and RISS. Nevertheless, recently Qian et al. (2001a, 2001c) have found that the polarization variations of IDV sources may contain important information on the nature of intraday variations and that multi-frequency observations of total flux density and linear polarization are very helpful for distinguishing different mechanisms, especially between intrinsic mechanisms and RISS.

In addition, VLBI polarization observations can be used to find rapid polarization variations in VLBI components and provide important clues to the mechanisms causing the IDV (Gabuzda & Kochanev 1997; Gabuzda et al. 1997; Kochanev & Gabuzda 1998, 1999). For example, Kochanev & Gabuzda (1998) observed two VLBI components in PKS 2155–152. One was variable in polarization on intraday timescales and the other was not. Interestingly the authors interpreted the intraday variations as being intrinsic to the source and on mas scales. This is consistent with the suggestion by Qian et al. (1991).

For the source 0917+624, some new results have recently been obtained. Fuhrmann et al. (2002) showed that the annual modulation on IDV timescale predicted by the scintillation model (Rickett et al. 2001; Qian & Zhang 2001b; Jauncey & Macquart 2001) is not confirmed by the observations during the period September 2000 – March 2001, indicating that the IDV behavior of the source is more complicated than expected. Krichbaum et al. (2002) showed that the change of the VLBI structure in 0917+624 may explain its IDV. Qian et al. (2001a, 2001c) analyzed the intraday variability of flux density and polarization at 20 cm and showed that there may be some intrinsic variations mixed with scintillation.

In this paper we will analyze the multi-frequency polarization behavior of 0917+624 and investigate the possibility for an interpretation in terms of the intrinsic shock model.

2 MULTI-FREQUENCY LIGHT-CURVES OF LINEAR POLARIZATION

For investigating the nature of IDV, multi-frequency observations of total flux density and linear polarization play an essential role. From these observations we can obtain the wavelength dependence of the variations including the timescale, modulation index, polarization behavior and correlations between the variations of polarized and total flux density, etc. and find some significant clues to the mechanisms responsible, because the wavelength dependence of these characteristics of the IDV is different for different mechanism. However, at present only a few IDV sources have been observed with high time-resolution at multiple frequencies in both total flux density and linear polarization (Wegner et al. 1996; Kraus et al. 1999a; Kedziora-Chudzcer et al. 1998; Quirrenbach et al. 2000); 0917+624 is one of these sources. Here we discuss two IDV events, which were observed in December 1988 (Julian Date 2447522–2447529) at 6 cm and 11 cm and in May 1989 (Julian Date 2447650–2447656)[1] at 20, 11, 6, 3.6 and 2 cm. In the following we designate them for brevity as the Dec88-event and the May89-event, respectively. In order to remove spurious rapid fluctuations caused by observational uncertainties, we took five-point running means for all the observed quantities. The measurement errors at the five wavelengths are then approximately as follows: for the total flux density: 3 mJy (20 cm), 10 mJy (11 cm), 3.5 mJy (6 cm), 7.5 mJy (3.6 cm) and 10 mJy (2 cm); for the polarized flux density: 0.75 mJy (20 cm), 0.65 mJy (11 cm), 0.25 mJy (6 cm), 0.4 mJy (3.6 cm) and 0.75 mJy (2 cm); for the polarization angle: 1.3° (20 cm), 1.5° (11 cm), 1° (6 cm), 1° (3.6 cm), 1.8° (2 cm).

[1] For brevity, a modified Julian Date (MJD), which is defined as MJD = Julian Date–2440000, will be used below.

2.1 The May89-event

2.1.1 Light-curves

The time curves of the total flux density, polarized flux density and polarization angle observed at 20 cm and the $Q-U$ track are shown in Fig. 1 and will be discussed in Section 2.1.2. The light-curves observed at the four higher frequencies and their $Q-U$ tracks are shown in Figures 6–9 and will be discussed in Section 2.1.3. Table 1 lists the mean values of the total flux density ($\bar{I}$), polarized flux density ($\bar{P}$), polarization angle ($\bar{\chi}$) and their variances (σ_I, σ_P, σ_χ), the mean values of the polarization degree ($\bar{p}$), the modulation indices of the fluctuations of the total and polarized flux density (m_I and m_P)[2].

Table 1 The May89-event

λ (cm)	$\bar{I}$ (Jy)	σ_I (Jy)	$\bar{P}$ (mJy)	σ_P (mJy)	$\bar{\chi}(^\circ)$	$\sigma_\chi(^\circ)$	$\bar{p}$ (%)	m_I (%)	m_P (%)
20	1.14	0.045	28.5	2.34	36.3	1.79	2.49	4.0	8.3
11	1.36	0.082	11.6	3.34	27.1	8.24	0.85	6.0	28.8
6	1.52	0.057	15.6	2.93	-5.8	8.71	1.03	3.8	18.8
3.6	1.57	0.032	18.0	1.58	-18.9	4.00	1.15	2.0	8.8
2	1.51	0.022	25.6	2.20	-18.9	3.61	1.70	1.4	8.6

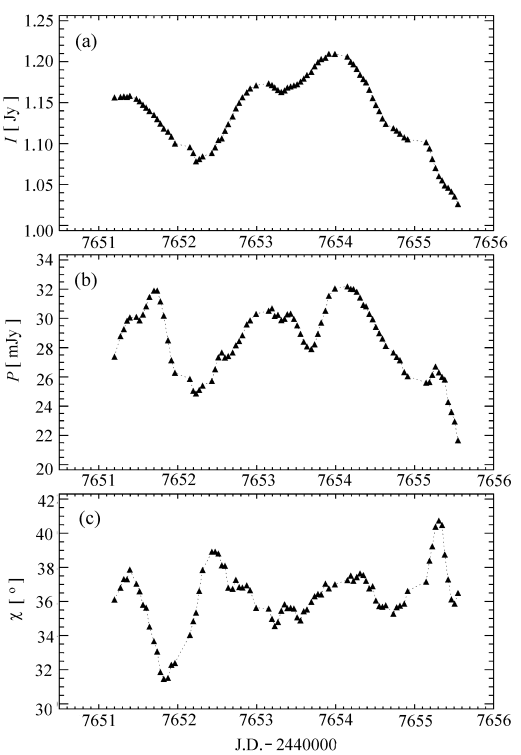

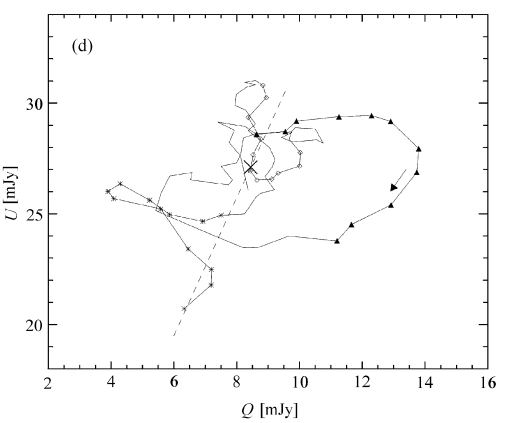

Fig. 1 The May89-event (20 cm): the observed light-curves of the total flux density I (in Jy), polarized flux density P (in mJy) and polarization angle χ (in deg) (a, b, c). In the Fig. 1d the solid curve represents the observed $Q-U$ track, and the dashed line is the fit to the observed polarization variation by the scintillation model proposed in Qian et al. (2001a). Symbols ∘, + and △ mark the segments for the three polarized features (see text).

[2] $m_I = \Delta I/\bar{I}$ and $m_P = \Delta P/\bar{P}$, ΔI and ΔP being the fluctuations of the total and polarized flux density, respectively.

From Table 1 it can be seen that the observed polarization degrees ($\bar{p}$) at all the five frequencies are very low (only $\sim 1-2\%$) and the amplitude of variation of the polarized flux density (m_P) is much larger than that (m_I) of the total flux density: the variations in polarization are more dramatic. Moreover, the polarization variation can help to resolve the sub-structures in the light-curves of the total flux density. For example, during the period MJD 7651.0–7652.0, the light-curves of the polarized flux density (see Figures 7–9) show that the flux density light-curves consist of two sub-structures with different polarizations. This characteristic is particularly useful for investigating the correlation between the variations at 1.4 GHz and at the higher frequencies (see below). Another interesting property is the increase of the mean polarization angle with wavelength (a rotation of about 50° from 2 cm to 20 cm). This could be due to different structures of the magnetic field in the source at different frequencies or an external Faraday rotation.

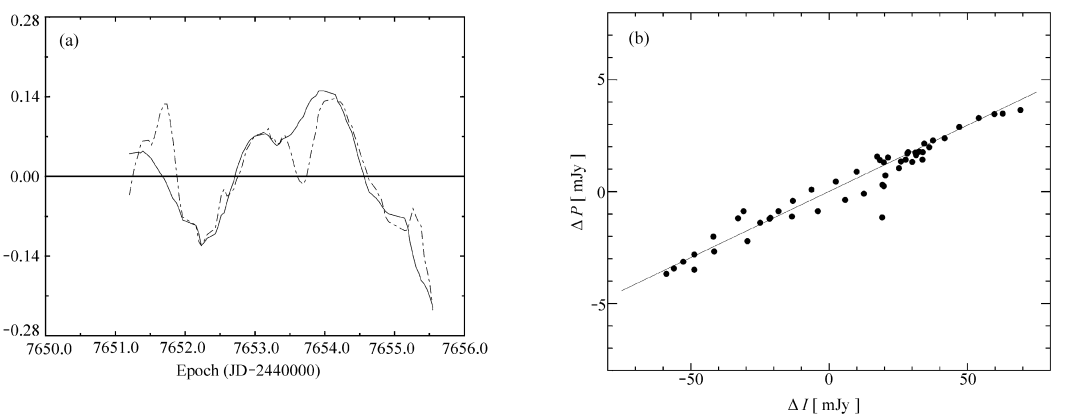

Fig. 2 (a) Observed fractional variations of the total flux density ($\Delta I(t)/\bar{I}$, solid line) and the polarized flux density ($\Delta P(t)/\bar{P}$, dot-dashed line) ($\bar{I} = 1.137$ Jy, $\bar{P} = 28.54$ mJy). The fractional variations of the total flux density have been scaled up by a factor 2.36. A clear correlation between ΔP and ΔI is visible. (b) Correlation between the polarized and total flux density (correlation coefficient 0.97).

2.1.2 Characteristics of the Event at 20 cm

Probably, the most important feature is that the variability pattern of the polarized flux density is highly dependent on the wavelength. This is most evident from a comparison between the polarized flux density variations at 20 cm and at the four higher frequencies.

It can be seen from Figure 1 that in the main part of the 20 cm light-curve (except the three time-intervals MJD 7651.5–7652.0, MJD 7653.5–7654.0 and MJD 7655.0–7655.5), the fractional variation of the polarized flux density is closely proportional to that of the total flux density and the polarization angle only varied slightly with a dispersion of $\sim 1.8°$ (Quirrenbach et al. 2000). This proportionality implies that refractive interstellar scintillation may be at work. These properties are essentially different from those observed at the higher frequencies, where we observed both correlation and anti-correlation between the variations of the polarized and

total flux densities and considerably larger variations of the polarization angle ($\sim 20^\circ - 40^\circ$).

The proportionality is shown in the right panel of Figure 2. It can be shown that in the case of one scintillating component, if $\Delta I \ll \bar{I}$ and $\Delta P \ll \bar{P}$, the proportionality between the fractional variations of the polarized and total flux density is approximately represented as:

$$\frac{\Delta P(t)}{\bar{P}} = \frac{p_2}{p_0} \cos(\chi_0 - \chi_2) \frac{\Delta I(t)}{\bar{I}} \,. \tag{1}$$

For the scintillation model proposed by Qian et al. (2001a), $\chi_0 \approx \chi_2$, the proportional coefficient is approximately equal to $\frac{p_2}{p_0} \approx 2.36$, which can be seen by an inspection of Figure 2. (Here the lower indices 0 and 2 refer to the background and scintillating component of the model respectively).

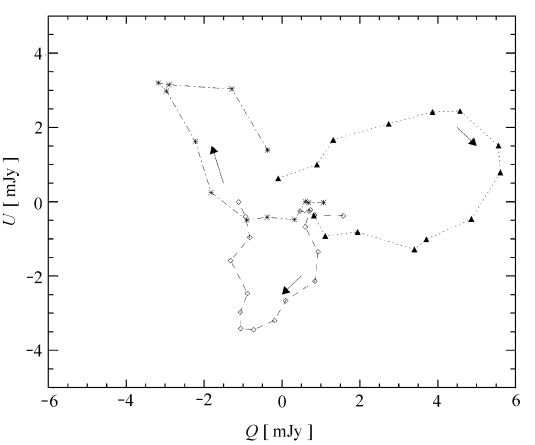

Fig. 3 The $Q-U$ tracks for the three 20 cm residual polarized features obtained when the variations due to scintillation were subtracted out. Symbols ∘, + and △ correspond to the respective segments in Figure 1 (right panel). The arrows indicate the direction of rotation of the polarization vector.

On the basis of the proportionality between the fractional variations of the polarized and total flux density observed at 20 cm, Qian et al. (2001a) have suggested that the intraday variations at this long wavelength are mostly caused by refractive interstellar scintillation. They showed that a two-component scintillation model (one steady background component and one scintillating component) can fit most of the polarized flux density light-curve extremely well. However, after subtracting the polarized flux density variations due to scintillation they found three "features" (feature-1 at MJD 7651.5–7652.0, feature-2 at MJD 7653.5–7654.0 and feature-3 at MJD 7655.0–7655.5) emerged in the 20 cm polarized flux density light-curve (Figure 2–3). Interestingly, feature-1 and feature-3 are correlated with the flux density minibursts at the higher frequencies, while feature-2 is anti-correlated with the minibursts. This result can be clearly seen from Figure 4, which compares the 20 cm polarized features and the variations of the total flux density at 2, 3.6, 6 and 11 cm. Taking into account the sub-structures in the variations of the total flux density at 11, 6 and 3.6 cm mentioned in Section 2.1.1, both the correlation and anti-correlation are evident, and the 20 cm features and the minibursts at the higher frequencies have almost the same durations of ~ 0.5 days. Figure 5 shows the cross-correlation function (CCF) between the 20 cm polarized feature-2 and the 6 cm intensity miniburst. It shows that the

CCF has a zero time lag and a minimum of ~ -0.7. For the other two 20 cm residual features the situation is similar. Therefore we are led to the conclusion that these 20 cm polarized features and the corresponding minibursts at the higher frequencies may be simultaneous variations and intrinsic to the source, because refractive interstellar scintillation cannot explain such broadband variations. For example, the refractive scintillation theory (Rickett et al. 1995; Walker 1998)

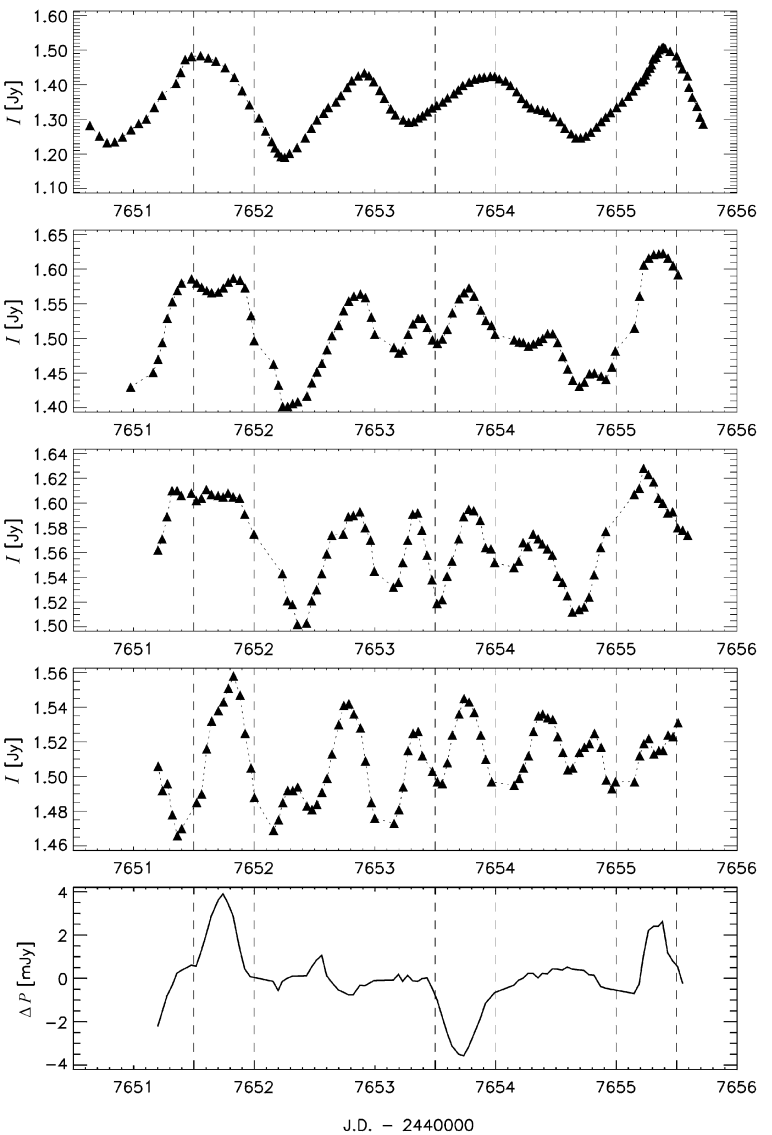

Fig. 4 Correlation and anti-correlation between the 20 cm polarized residuals (at MJD 7651.5–7652.0, MJD 7653.5–7654.0 and MJD 7655.0–7655.5) and the total flux density variations at (from top to bottom) 11 cm, 6 cm, 3.6 cm, 2 cm and 20 cm.

predicts that the timescale of scintillation at 2 cm and 20 cm should differ by a factor of ∼10, which is contrary to the observations. In addition, the $Q-U$ tracks of the three residual features are distributed in different sections in the $Q-U$ plane with an angular separation of $\sim 120^\circ$ (see Figure 3). This distribution cannot be caused by another scintillating component, because the presence of such a component would destroy the precise proportionality between the fractional variations of the polarized and total flux density. Moreover, the $Q-U$ track caused by this component would be another straight line in the $Q-U$ plane, which could not fit the widely separated $Q-U$ tracks of the three residual features.

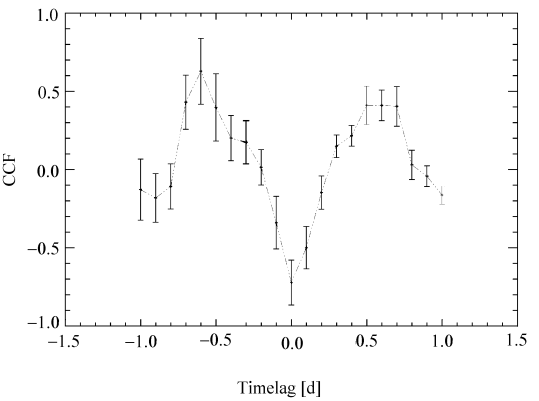

Fig. 5 The cross-correlation function between the 20 cm polarized feature-2 (MJD 7653.5 – 7654.0) and the flux density miniburst at 6 cm.

Therefore, we come to the conclusion that the 20 cm residual features and most or part of the associated variations at the higher frequencies may be intrinsic to the source, i.e., scintillation may be a secondary effect at the higher frequencies. This provides a fairly strong physical basis for considering intrinsic models for the IDV events observed in this source.

For the detailed analysis of the scintillation model for the 20 cm variations of the polarized and total flux density and the separation of the intrinsic variations from scintillation, see Qian et al. (2001a, 2001c). In this paper we concentrate on the analysis of the polarization variations at the high frequencies in terms of shock models.

2.1.3 Characteristics of the event at high frequencies

From Figures 6–9, it can be seen that at the four high frequencies ($\nu \geq 2.7$ GHz), the prominent features of the event may be the correlation and anti-correlation between the variations of the polarized and total flux density, and the rapid transition between these two states. The most complicated variability appears in the polarized flux density at 6 cm (Figure 7), where the correlation between the variations of the polarized flux density and the total flux density was positive in some intervals and negative in other intervals, and the transition between the two states was very rapid (timescale of < 0.5 days), for example, in the interval MJD 7652.5–7653.5. In addition, in some periods the total flux density changed only a little, but the polarized flux density changed greatly (for example in the interval MJD 7654.60–7654.90). The opposite behaviour was also observed in some cases.

Moreover, the properties of the polarization variations are significantly different for different wavelengths, although the total flux density variations at the four high frequencies were well correlated. For example, during the period MJD 7653.0–7654.0 the polarized flux density is correlated with the total flux density at 6 cm, but at 2 cm they are anti-correlated. At 11 cm the polarized flux density was more often anti-correlated with the total flux density. Intraday polarization variability with a strong dependence on wavelength has been observed in other sources, for example in 1150+812 (Kochanev & Gabuzda 1999): a rapid polarization angle swing of $\sim 180^\circ$ was observed at 2 cm, but at 3.6 cm no PA swing occurred.

2.2 The Dec88-event

2.2.1 Light-curves

The light-curves of the Dec88 event observed at 11 and 6 cm of the total flux density, polarized flux density and polarization angle are shown in Figures 10–11, respectively. The mean values of the total flux density ($\bar{I}$), polarized flux density ($\bar{P}$), polarization angle ($\bar{\chi}$) and their variances (σ_I, σ_P, σ_χ), the mean values of the polarization degree ($\bar{p}$) and the modulation indices of the fluctuations of the total and polarized flux density (m_I, m_P) are listed in Table 2. It is evident that the main parameters of this event are similar to those of the May89-event.

Table 2 The Dec88-event

λ (cm)	$\bar{I}$ (Jy)	σ_I (Jy)	$\bar{P}$ (mJy)	σ_P (mJy)	$\bar{\chi}$ ($^\circ$)	σ_χ($^\circ$)	$\bar{p}$(%)	m_I(%)	m_P(%)
11	1.24	0.087	10.6	1.9	49.5	6.0	0.85	7.0	18.2
6	1.43	0.079	12.4	3.0	18.4	11.7	0.86	5.5	24.5

2.2.2 Characteristics of the event

It can be seen from Figures 9–10 that anti-correlated variations often occurred between the polarized and total flux densities, especially at 6 cm. However, probably the most prominent feature of this event is the rapid polarization angle swing of $\sim 180^\circ$ observed at 6 cm during the period ∼MJD 7525.75–7526.25 ($\sim$ 0.5 days, Figure 10). At 11 cm, no corresponding PA swing occurred. This rapid polarization angle swing could not be explained in terms of scintillation by a continuous interstellar medium and was suggested to be due to "low-level" intrinsic variations (Rickett et al. 1995). Simonetti (1992) proposed a specific model of refractive focusing by an interstellar shock moving across the line of sight to explain the PA swing, but it is not clear how this shock affects the entire event. Qian et al. (1991) suggested an interpretation of this PA swing together with the other distinct variations of polarization in an unified scheme by using a two-component shock model. They found that the polarization orientation of the shock component should be approximately perpendicular to that of the background component. This is required by the anti-correlation between the variations of the total and the polarized flux density observed in most of the light-curves. They also demonstrated that the polarization degree and polarization angle of the shock component are required to vary only within a narrow range. In addition, this PA swing event occurred when the polarized flux density was at minimum. This phenomenon is quite similar to the PA swings with longer timescales (weeks or months) in active compact radio sources, which can usually be interpreted as a random walk process in a turbulent jet with a random magnetic field (Jones et al. 1985).

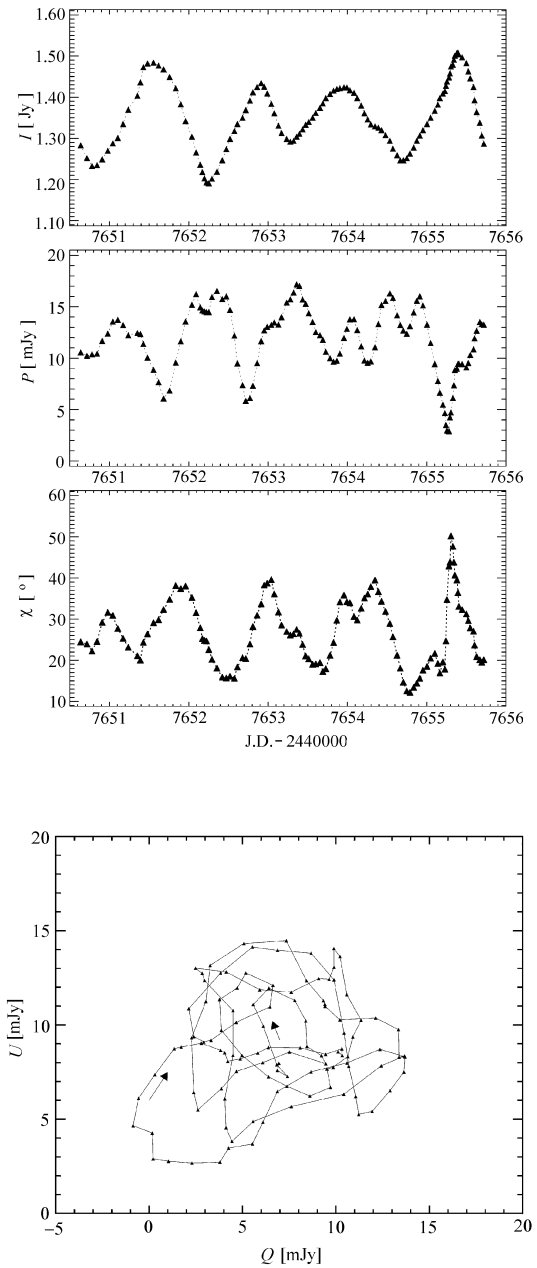

Fig. 6 The May89-event (11 cm): the observed light-curves of the total flux density I (in Jy), polarized flux density P (in mJy) and polarization angle χ (in deg). The lowest panel shows the observed $Q-U$ track.

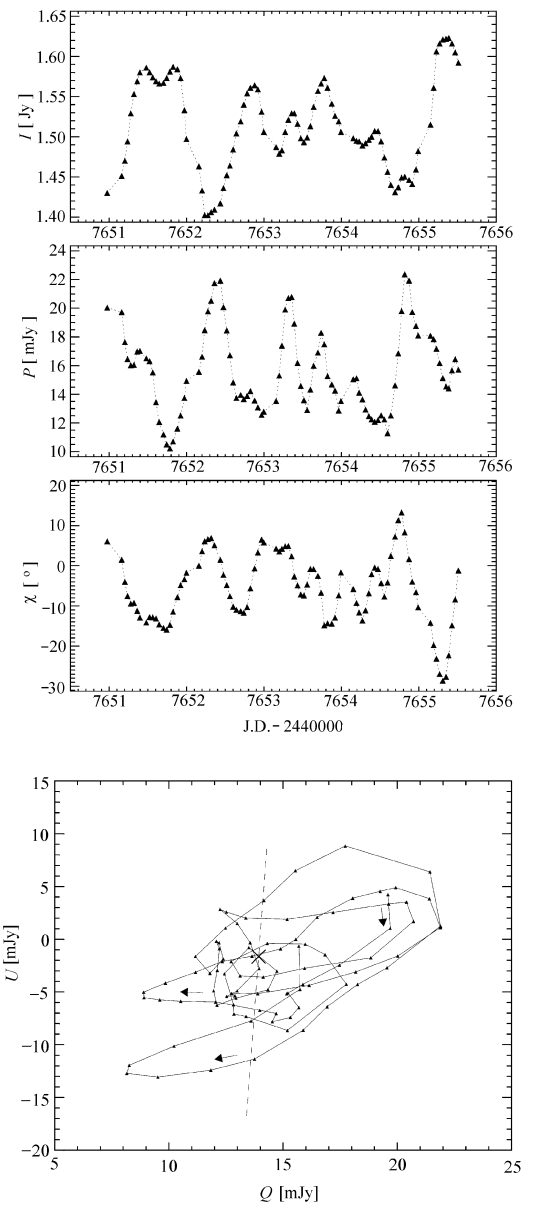

Fig. 7 The May89-event (6 cm): the observed light-curves of the total flux density I (in Jy), polarized flux density P (in mJy) and polarization angle χ (in deg). The lowest panel shows the observed $Q-U$ track. The dashed straight line is the fit by a scintillation model with one scintillating component (from Rickett et al. 1995).

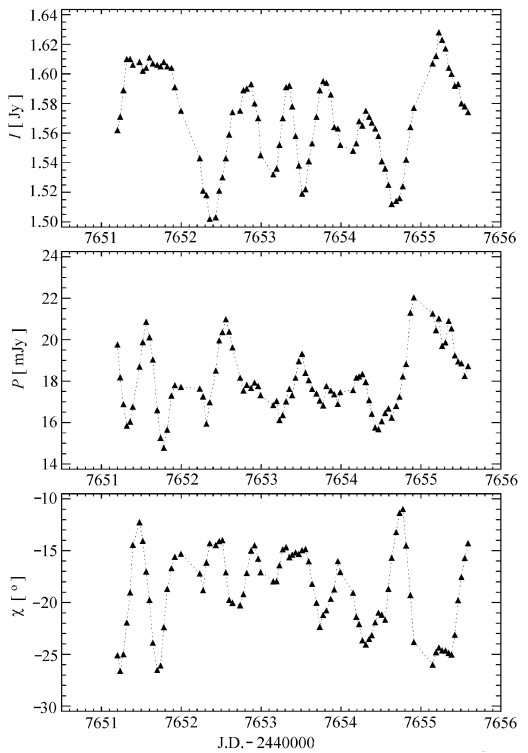

Fig. 8 The May89-event (3.6 cm): the observed light-curves of the total flux density I (in Jy), polarized flux density P (in mJy) and polarization angle χ (in deg). The lowest panel shows the observed $Q-U$ track.

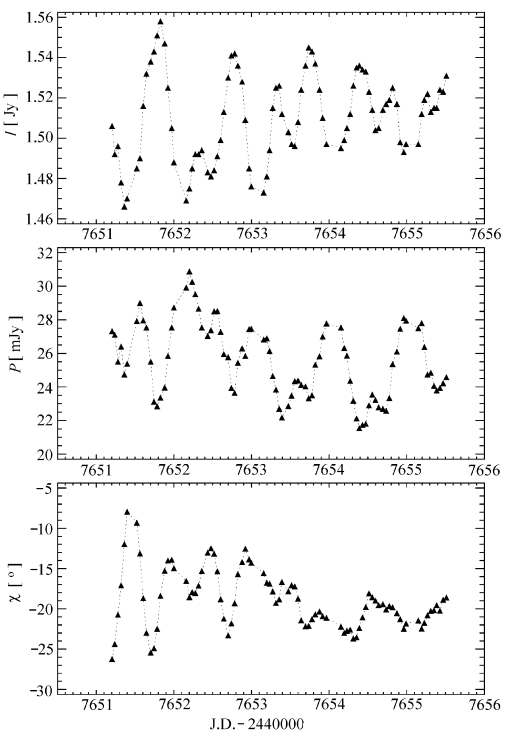

Fig. 9 The May89-event (2 cm): the observed light-curves of the total flux density I (in Jy), polarized flux density P (in mJy) and polarization angle χ (in deg). In the lowest panel is shown the observed $Q-U$ track.

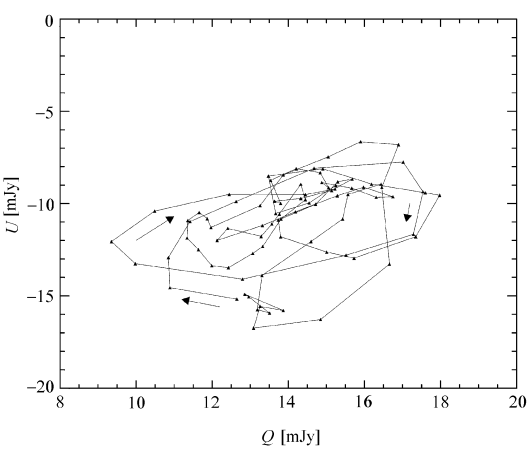

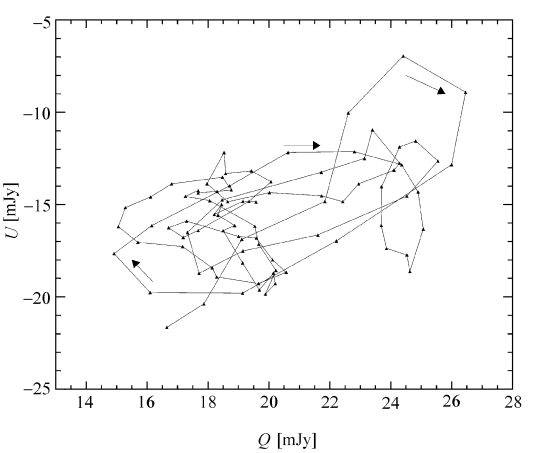

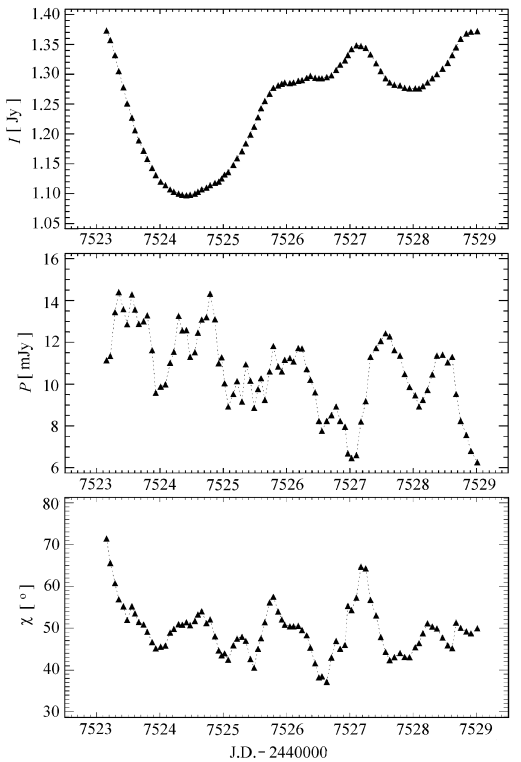

Fig. 10 The Dec88-event (11 cm): the observed light-curves of the total flux density, polarized flux density and polarization angle. In the lowest panel is shown the observed $Q-U$ track.

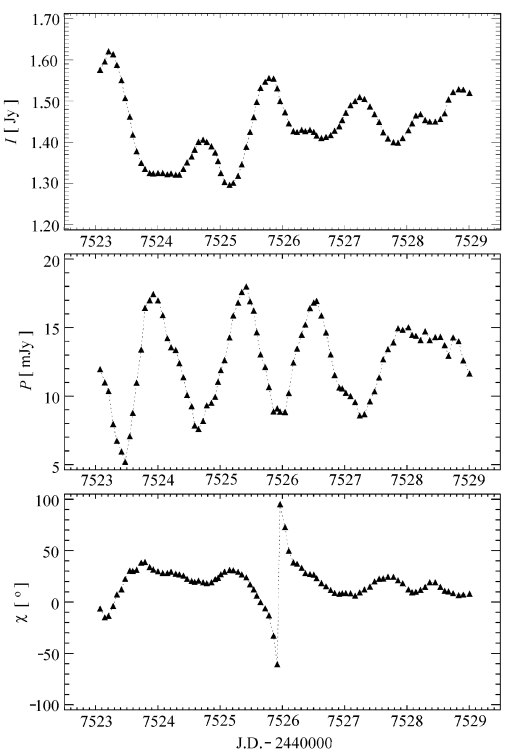

Fig. 11 The Dec88-event (6 cm): the observed light-curves of the total flux density, polarized flux density and polarization angle. In the lowest panel, the curve represents the observed $Q-U$ track and the dotted arc-segment marks the observed rapid polarization angle swing of $\sim 180°$. The dashed line is the fit to the observed polarization variation by the scintillation model proposed by Rickett et al. (1995). It is clear that the rapid swing cannot be explained by the scintillation model.

2.3 Brief Discussion

In summary, the multi-frequency polarization behavior of the intraday variations of the two events observed in 0917+624 has provided some important information about the origin of the IDV, information that especially helps to separate the intrinsic variations from the refractive interstellar scintillation and to underline that intrinsic mechanisms are required for the explanation of the intraday variations at centimeter wavelengths in this source. The complicated multifrequency polarization behavior calls for a unified scheme that explains properties ranging from the rapid PA swing to the correlation between the total flux density and linear polarization in a wide range of wavelength.

3 SHOCK MODEL

3.1 Introduction

As we argued above from the analysis of the multi-frequency polarization observations, the intraday variations at the high frequencies (from 2.7 GHz to 15 GHz) observed in 0917+624 may be mainly (or at least partly) intrinsic. This is supported by the recent work on the correlation between the 20 cm residual polarized features and the variations of the flux density at the higher frequencies (Qian et al. 2001a, 2001c). Therefore, the multi-frequency polarization behavior of this event, like that for the Dec88-event (Qian et al. 1991), may also be explained in terms of some shock model. Most of the shock models proposed in the literature (Qian et al. 1991; Marscher 1992, 1996; Gopal–Krishna & Wiita 1992; Spada et al. 1999; etc.), emphasise the importance of the relativistic effects (Doppler beaming, relativistic aberration, light-travel-time effects).

In the following we will use the shock model proposed by Qian et al. (1991) to investigate further the multi-frequency polarization behavior of the IDV events observed in 0917+624. In doing so, we make the assumption that at the high frequencies refractive interstellar scintillation is negligible in order to present a unified description and show the essential properties of the shock model.

3.2 Basic Equations

In the case of two-component shock model the basic equations for the Stokes parameters are

$$I(t) = I_0 + I_v(t), \tag{2}$$

$$Q(t) = Q_0 + I_v(t) \cdot m_q(t), \tag{3}$$

$$U(t) = U_0 + I_v(t) \cdot m_u(t), \tag{4}$$

$$Q_0 = I_0 \cdot p_0 \cdot \cos 2\chi_0, \tag{5}$$

$$U_0 = I_0 \cdot p_0 \cdot \sin 2\chi_0, \tag{6}$$

$$m_q(t) = p_v(t) \cdot \cos 2\chi_v(t), \tag{7}$$

$$m_u(t) = p_v(t) \cdot \sin 2\chi_v(t), \tag{8}$$

where $(I(t), Q(t), U(t))$ are the observed Stokes parameters, (I_0, Q_0, U_0) are the Stokes parameters of the steady background component, p_0 and χ_0 are its degree and angle of polarization, $I_v(t)$, $p_v(t)$, and $\chi_v(t)$ are the flux density, polarization degree and angle of the shock compo-

nent. These three sets of parameters are functions of time and are related to the propagation of the shock through the jet plasma.

In order to use the shock model to study the intraday variations, we should first separate the flux density of the background component from the observed total flux density. For this, we have to refer to the source structures measured at multiple frequencies with VLBI (Standke et al. 1996). As shown by Qian et al. (1996), if the shock component is assumed to be a homogeneous synchrotron source, then for the event of May 1989 the appropriate values for I_0 at the four frequencies are: 1.26 Jy (15 GHz), 1.23 Jy (8.3 GHz), 1.00 Jy (5.0 GHz) and 1.00 Jy (2.7 GHz). We will use these values also for the event of December 1988.

Having chosen the flux density of the background component we can obtain the flux density light-curves $I_v(t)$ of the shock component for the four frequencies, then we solve Eqs. (2) and (3) to obtain (Q_0, U_0) and $m_q(t)$ and $m_u(t)$. However, the latter two items are functions of time, so usually the equations cannot be solved. However, as Qian et al. (1991) have shown, in the scenario of shock models the degree of polarization $p_v(t)$ and the angle of polarization $\chi_v(t)$ only vary in very narrow ranges, therefore we can deal with the solution for (Q_0, U_0) as follows. In each of the flux density light-curves we select a short period in which the flux density varies rapidly. We assume that within this period the variation of the polarization is caused only by the variation of the flux density from the shock, and the polarization degree and angle of the shock remain constant. In this way the approximate values for (Q_0, U_0) (and therefore p_0 and χ_0) for each of the frequencies can be determined. Then we substitute these values into the equations (2) and (3) to obtain the polarization degree $p_v(t)$ and polarization angle $\chi_v(t)$ for the shock component for the complete observed light-curves. Obviously, the solution for $p_v(t)$ and $\chi_v(t)$ obtained by using such a procedure is not unique, but is reasonable and adequate for our investigation of the properties of the shock component, because what we are mostly concerned with is the range of variability of the degree and angle of polarization of the shock, rather than their absolute values.

3.3 The May89-event

For this event the time intervals chosen for determining the parameters (Q_0, U_0, p_0, χ_0) of the background component are: 7651.828–7652.160 (2 cm), 7652.517–7652.822 (3.6 cm), 7651.883–7652.201 (6 cm) and 7651.682–7652.040 (11 cm). The results for the four frequencies are given in Table 3 and the model light-curves of the polarization degree and polarization angle obtained for the shock component are shown in Figures 12–15. The corresponding parameters (the mean values of the flux density ($\bar{I_v}$), polarization degree ($\bar{p_v}$), polarization angle ($\bar{\chi_v}$)) and their variations (σ_{I_v}, σ_{p_v} and σ_{χ_v}) are given in Table 4.

Table 3 The May89-event: the Model Parameters for the Background Component

λ (cm)	I_0 (Jy)	Q_0 (mJy)	U_0 (mJy)	p_0 (%)	χ_0 ($^\circ$)
11	1.000	9.63	30.7	3.21	36.3
6	1.000	31.6	17.0	3.59	14.1
3.6	1.230	34.3	−7.1	2.84	−5.86
2	1.260	40.0	−21.8	3.62	−14.3

It can be seen: (1) that the polarization degree p_0 of the background component is very low ($\sim 3\%$) for all the four frequencies; (2) that the polarization angle χ_0 continuously rotates by

about 50° from 2 cm to 11 cm; (3) that the polarization degree of the shock component $\bar{p_v}$ is $\sim 5-8\,\%$ and varies in a narrow range ($m_{p_v} = \sigma_{p_v}/\bar{p_v} \sim 0.10-0.25$); (4) that the polarization orientation of the shock component is approximately perpendicular to that of the background component for all the four frequencies (i.e. $\bar{\chi_v} - \chi_0 \approx 90°$). Thus the polarization position angle of the shock component also rotates $\sim 50°$ between 2 cm and 11 cm. This result may imply a rotation of the magnetic field structure in the IDV component (or jet); (5) that the polarization position angle of the shock component varies in a very narrow range for all the four frequencies ($\sigma_{\chi_v} \sim 3-5°$).

These results show that when the polarization orientation of the shock component is approximately perpendicular to that of the background component, small changes of the polarization degree and the polarization angle of the shock component can well reproduce the complicated polarization variations observed in this IDV event, including the correlation and anti-correlation between the total and the polarized flux density, the rapid transition between the two states and the other properties.

Table 4 The May89-event: the Model Parameters for the Shock Component

λ (cm)	$\bar{I_v}$ (Jy)	σ_{I_v} (Jy)	$\bar{p_v}$	σ_{p_v}	$\bar{\chi_v}$ (°)	σ_{χ_v} (deg)	m_{I_v} (%)	m_{p_v} (%)	$\bar{\chi_v} - \chi_0$ (°)
11	0.358	0.0815	0.0654	0.0156	132.5	4.60	22.8	23.9	96.2
6	0.515	0.0572	0.0505	0.0067	114.4	3.03	11.1	13.3	100.3
3.6	0.340	0.0316	0.0611	0.0065	95.3	2.98	9.3	10.6	101.2
2	0.250	0.0215	0.0845	0.0072	81.0	4.30	8.6	8.5	95.3

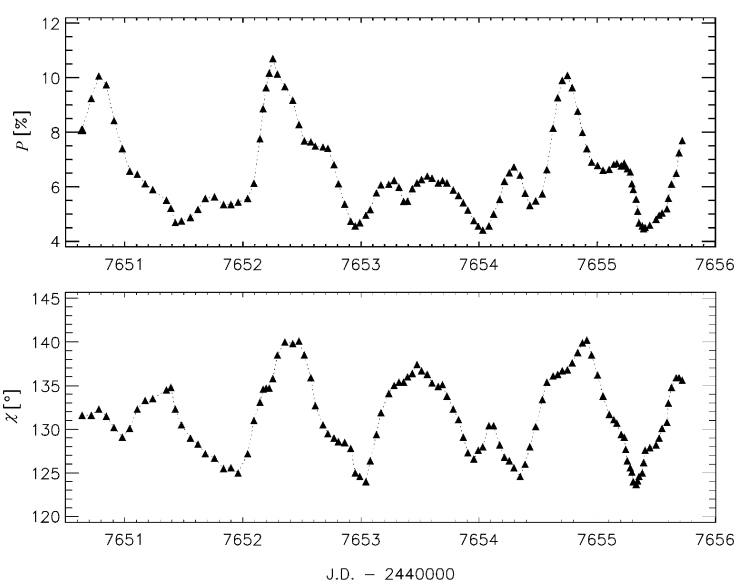

Fig. 12 The May89-event: the model light-curves of the polarization degree and polarization angle of the shock component at 11 cm.

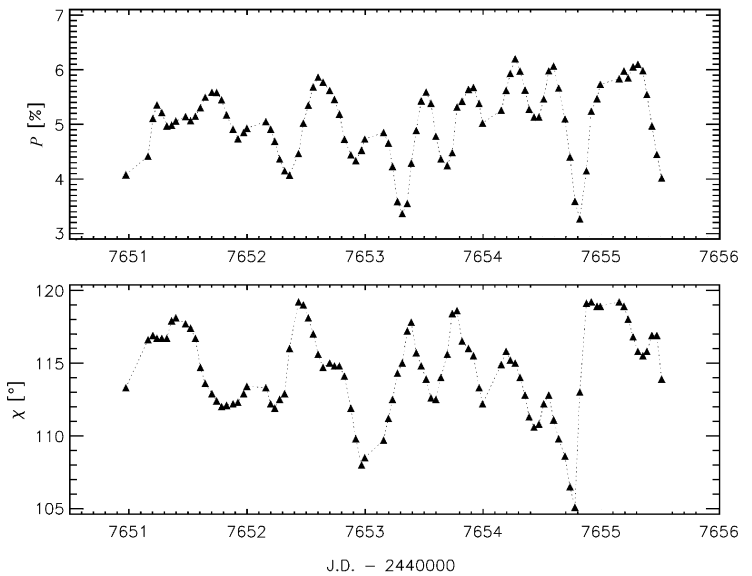

Fig. 13 The May89-event: the model light-curves of the polarization degree and polarization angle of the shock component at 6 cm.

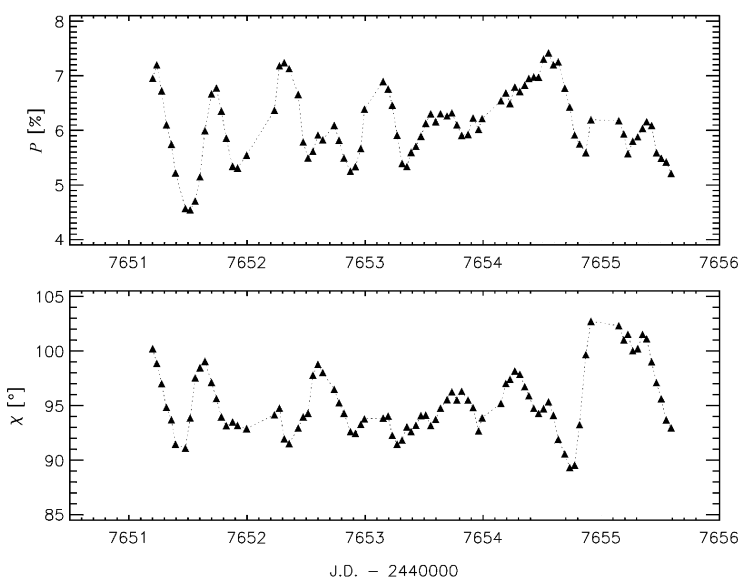

Fig. 14 The May89-event: the model light-curves of the polarization degree and polarization angle of the shock component at 3.6 cm.

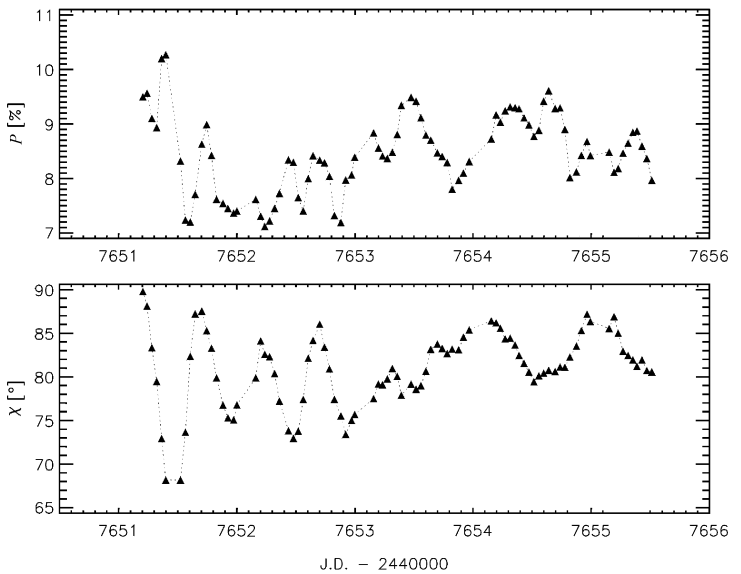

Fig. 15 The May89-event: the model light-curves of the polarization degree and polarization angle of the shock component at 2 cm.

3.4 The Dec88-event

Similarly, for this event the parameters (Q_0, U_0) of the background component and the polarization degree p_v(t) and polarization angle χ_v(t) of the shock component are determined for the two frequencies. The time intervals chosen for determining (Q_0, U_0) are: 7523.417–7523.794 (6 cm) and 7523.558–7523.935 (11 cm). The model light-curves of p_v(t) and χ_v(t) of the shock component are shown in Figures 16–17, respectively. The model parameters for the background component are listed in Table 5 and the mean values of the parameters for the shock component and their variations are listed in Table 6. For this event the derived parameters for both the background component and shock component (p_0, χ_0, $\bar{p_v}$, $\bar{\chi_v}$, etc.) are similar to those derived for the May89-event. The polarization orientation of the shock component is also approximately perpendicular to that of the background component. As we already pointed out, in this event the most prominent features are the rapid polarization angle swing at 6 cm during the interval ∼MJD 7525.75–7526.25 (see Figure 11) and the anti-correlated variations of the polarized and total flux density. It can be seen from Figure 17 that, in the shock model the rapid PA swing of $\sim 180^\circ$ does not require any special conditions. The only "abnormal" behavior is that during the period of the PA swing the polarization angle of the shock component has a slightly larger deviations ($\sim 15^\circ$ or more) from the mean value. This shows once again that the shock model is very flexible in fitting the polarization behavior of IDV events.

Another feature of this event is that at 11 cm during the interval MJD 7524.0–7524.5 the polarization degree derived for the shock component is much higher than the mean value (by a factor ∼2). This is because during this period the observed total flux density is extremely

low while the polarized flux density is high (see Figure 10). It can be seen from Table 6 that in comparison with the May89-event the polarization variations at 11 cm of this event require much higher values of m_{p_v} and m_{I_v} for the shock component and the difference of the polarization angle between the shock component and the background component $\bar{\chi_v} - \chi_0$ is $\sim 57^\circ$. These properties differ significantly from the May89-event at 11 cm. It is possible that in this event scintillation has a significant contribution at 11 cm.

Table 5 The Dec88-event: the Model Parameters for the Background Component

λ (cm)	I_0 (Jy)	Q_0 (mJy)	U_0 (mJy)	p_0 (%)	χ_0 ($^\circ$)
11	1.000	6.7	4.4	0.8	16.6
6	1.000	0.47	37.1	3.71	44.6

Table 6 The Dec88-event: the Model Parameters for the Shock Component

λ (cm)	$\bar{I_v}$ (Jy)	σ_{I_v} (Jy)	$\bar{p_v}$	σ_{p_v}	$\bar{\chi_v}$ ($^\circ$)	σ_{χ_v} ($^\circ$)	m_{I_v} (%)	m_{p_v} (%)	$\bar{\chi_v} - \chi_0$ ($^\circ$)
11	0.245	0.0871	0.0524	0.0303	73.2	5.03	35.6	57.8	56.6
6	0.435	0.0795	0.0742	0.00793	144.0	4.11	18.3	10.7	99.4

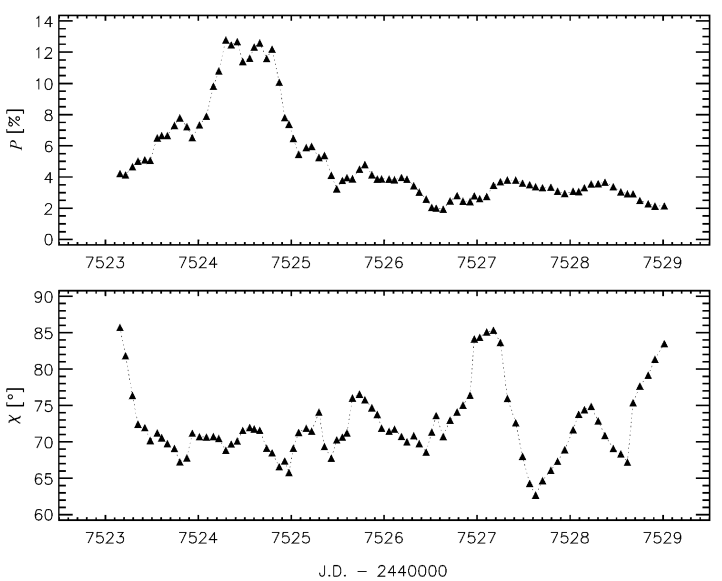

Fig. 16 The Dec88-event: the model light-curves of the polarization degree and polarization angle of the shock component at 11 cm.

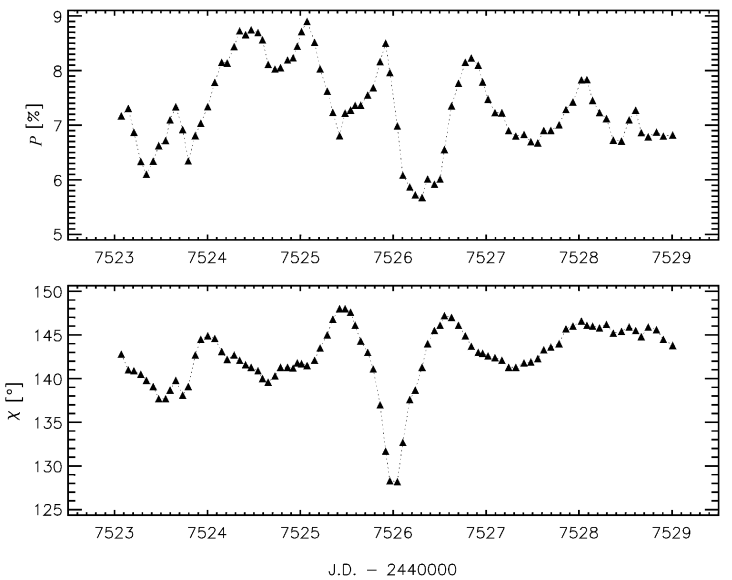

Fig. 17 The Dec88-event: the model light-curves of the polarization degree and polarization angle of the shock component at 6 cm.

4 DISCUSSION

We have shown that the intraday variations in 0917+624 of both the total flux density and linear polarization are highly wavelength-dependent. Thus multifrequency observations of flux density and linear polarization are very useful for studying the origin of IDV. However, for distinguishing intrinsic mechanisms from refractive interstellar scintillation, such observations should cover a very broad waveband. A good example is the separation of the intrinsic variations from scintillation for the May89-event, for which the multifrequency observations were carried out in a waveband from 2 cm to 20 cm. Only in this case is the different polarization behavior at 20 cm and at the higher frequencies revealed.

From the analysis of the two IDV events in 0917+624 we can see that the intraday polarization variations are quite complicated. The characteristics of the polarization behavior can be summarized as follows:

— More dramatic variations in polarization (polarization degree and polarization angle) than in total flux density;
— both correlation and anti-correlation between the variations of the polarized and total flux density;
— fast transition between the correlation and anti-correlation;
— rapid polarization angle swing of $\sim 180^\circ$;
— fast variations of the polarized flux density together with little variation of the total flux density;

— fast variations of the total flux density together with little variation of the polarized flux density;

— different behavior of polarization variations at different frequencies.

As shown above, all these features can be well interpreted in terms of a two component shock model. The main characteristic of the shock model is that both the degree and angle of polarization of the shock component are rapidly variable. This is related to the assumption that the shock is propagating in the jet, in which the synchrotron-emitting electrons and magnetic field (both magnitude and direction) are largely turbulent (Qian et al. 1991; Marscher 1992, 1996). In such a case large PA swings can occur through a random walk process as suggested by Jones et al. (1985). We have shown that, when the polarization orientation of the shock component is approximately perpendicular to that of the background component, all the observed features of the polarization variations in 0917+624 can be explained and the degree of polarization and polarization angle of the shock component are required to vary only in a rather narrow range. Thus, for the explanation of the intraday polarization variations in 0917+624 the shock model proposed in this paper is very flexible.

The intraday polarization variations at 6 cm of the two events have also been explained in terms of a scintillation model (Rickett et al. 1995). The main characteristic of the scintillation model is that any individual scintillating component keeps the degree and angle of polarization constant while the flux density fluctuates (or scintillates). Thus, the observed polarization variations are caused by the fluctuations of the polarized flux density of the scintillating component. The observed polarization is the vector sum of the polarizations from the scintillating and background (non-scintillating) component. (Here we discuss the simple case of only one scintillating component). Therefore, within the scintillation scenario, a scintillating component, which produces correlated variations of total and polarized flux density, cannot produce anti-correlated variations, and vice versa. So rapid transition between the correlation and anti-correlation would require a "coordinated" variation of two scintillating components. Similarly a single scintillating component, which can produce correlated or anti-correlated variations, cannot produce rapid polarization angle swings. In addition, large polarized flux density variations with small variations of total flux density (or small variations of polarized flux density with large variations of total flux density) cannot be explained by one scintillating component. Scintillation models with multiple scintillating components might be capable to explain the general pattern of the complicated polarization variations in 0917+624 (except the rapid polarization angle swing), but these models do not seem to be able to clarify the simultaneous polarization variations at 20 cm and at 2–6 cm.

The difference between the shock model and scintillation model in explaining intraday polarization variations is essential. In order to distinguish these two models, more multifrequency observations of total flux density and linear polarization are desirable, especially at both long ($\sim$20 cm) and short wavelengths ($\leq 2-6$ cm). VLBI polarization observations can find the components causing intraday variations and measure their angular sizes (and apparent brightness temperatures). This is also important for disclosing the nature of the radio IDV phenomenon (Kochanev & Gabuzda 1999; Gabuzda & Kochanev 1997).

Acknowledgements We thank I. I. K. Pauliny−Toth for critically reading the manuscript and valuable comments. SJQ acknowledges the support from Max-Planck-Institut für Radioastronomie during his visit (1999–2000).

References

Begelman M. C., Rees M. J., Sikora M., 1994, ApJ, 429, L57

Coppi P., 1997, In: M. Ostrowski, M. Sikora, G. Madejski, M. Begelman, eds., Relativistic Jets in AGNs, Towarzystwa Salezjanskiego: Krakow, p.333

Dennett-Thorpe J., de Bruyn A. G., 2000, ApJ, 529, L65

Fuhrmann L., Krichbaum T. P., Cimo G., Beckert T., Kraus A., Witzel A., Zensus J. A., Qian S. J., Rickett B. J., 2002, Proc. Astron. Soc. Aust., 19, 64

Gabuzda D. C., Kochanev P. Yu., 1997, Vistas of Astronomy, 2, 219

Gabuzda D. C., Kochaev P. Yu., Kollgaard R. I., 1998, In: J. A. Zensus, G. B. Taylor, J. M. Wrobel, eds., Radio Emission From Galactic and Extragalactic Compact Sources, San Francisco: ASP, p.265

Gabuzda D. C., Kochenov P. Yu., Cawthorne T. V., Kollgaard R. I., 1999, In: L. O. Takalo, A. Sillanpää, eds., BL Lac Phenomenon, San Francisco: ASP, p.447

Gopal-Krishna, Wiita P. J., 1992, A&A, 259, 109

Heeschen D. S., Krichbaum T. P., Schalinski C. J., Witzel A., 1987, AJ, 94, 1493

Jauncey D. L., Macquart J. -P., 2001, A&A, 370, L9

Kedziora-Chudzcer L., Jauncey D. L., Wieringa M. H. et al., 1997, ApJ, 490, L9

Kedziora-Chudzcer L., Jauncey D. L., Wieringa M. H. et al., 1998, BAAS, 30, 903

Kellermann K. I., Pauliny-Toth I. I. K., 1969, ApJ, 155, L71

Kochanev P. Yu., Gabuzda D. C., 1999, In: L. O. Takalo, A. Sillanpää, eds., ASP Con. Ser. Vol. 159, BL Lac Phenomenon, San Francisco: ASP, p.460

Kochanev P. Yu., Gabuzda D. C., 1998, In: J. A. Zensus, G. B. Taylor, J. M. Wrobel, eds., Radio Emission From Galactic and Extragalactic Compact Sources, San Francisco: ASP, p.273

Kraus A., Krichbaum T. P., Witzel A., 1999a, L. O. Takalo, A.Sillanpää, eds., ASP Con. Ser. Vol. 159, BL Lac Phenomenon, San Francisco: ASP, p.49

Kraus A., Witzel A., Krichbaum T. P., Peng B., 1999b, A&A, 352, L107

Krichbaum T. P., Kraus A., Fuhrmann L., Cimo G., Witzel A., 2002, Proc. Astron. Soc. Austr., 19, 14

Jones T. W., Rudnick R., Aller H. D. et al., 1985, ApJ, 290, 627

Marscher A. P., 1992, In: W. J. Duschl, S. J. Wagner, eds., Physics of Active Galactic Nuclei, Berlin: Springer-Verlag, p.510

Marscher A. P., 1996, In: J. G. Kirk, M. Camenzind, C. von Montigny, S. Wagner, eds., Proceedings of the Heidelberg Workshop on Gamma-ray Emitting AGN, MPIfK: Heidelberg, p.103

Qian S. J., Quirrenbach A., Witzel A., Krichbaum T. P., Hummel C. A., Zensus J. A., 1991, A&A, 241, 15

Qian S. J., 1994a, Acta Astron. Sin., 35, 362 (Transl.: Chin. Astron. Astrophys., 1995, 19, 267)

Qian S. J., 1994b, Acta Astrophys. Sin., 14, 333 (Transl.: Chin. Astron. Astrophys., 1995, 19, 69)

Qian S. J., Britzen S., Witzel A. et al. 1995, A&A, 295, 47

Qian S. J., Li X. C., Wegner R., Witzel A., Krichbaum T. P., 1996, Chin. Astron. Astrophys., 20, 15

Qian S. J., Britzen S., Witzel A. et al., 1996, In: P. E. Hardee, A. H. Bridle, J. A. Zensus, eds., Energy Transport in Radio Galaxies and Quasars, ASP Con. Ser. Vol. 100, San Francisco: ASP, p.55

Qian S. J., Witzel A., Kraus A., Krichbaum T. P., Zensus J. A., 2001a, A&A, 367, 770

Qian S. J., Zhang X. Z., 2001b, Chin. J. Astron. Astrophys. 1, 133

Qian S. J., Kraus A., Krichbaum T. P., Witzel A., Zensus J. A., 2001c, Ap&SS, 278, 119

Quirrenbach A., Witzel A., Wagner S. et al. 1991, ApJ, 372, L71

Quirrenbach A., Witzel A., Qian S. J., Krichbaum T. P., Hummel C. A., Alberti A., 1989, A&A, 226, L1

Quirrenbach A., Kraus A., Witzel A. et al., 2000, A&AS, 141, 221
Rickett B. J., 1990, ARA&A, 28, 561
Rickett B. J., Quirrenbach A., Wegner R., Krichbaum T. P., Witzel A., 1995, A&A, 293, 479
Rickett B. J., Witzel A., Kraus A., Krichbaum T. P., Qian S. J., 2001, ApJ, 550, L11
Rickett B. J., 2002, Proc. Astron. Soc. Aust., 19, 100
Simonetti H. J., 1992, A&A, 250, L1
Spada M., Salvati M., Pacini F., 1999, In: L. O. Takalo, A. Sillanpää, eds., ASP Con. Ser. Vol. 159, BL Lac Phenomenon, San Francisco: ASP, p.464
Standke K. J., Quirrenbach A., Krichbaum T. P. et al., 1996, A&A, 306, 27
Wagner S., Witzel A., 1995, ARA&A, 33, 163
Wagner S. J., Witzel A., Heidt J., Krichbaum T. P., Qian S. J. et al., 1996, AJ, 111, 2187
Walker M. A., 1998, MNRAS, 294, 307
Wegner R., 1994, Kurzzeitvariabilität der Intensität und Polarisation Aktiver Galaxienkerne (Dissertation), Max-Planck-Institut für Radioastronomie, Bonn, Germany
Witzel A., 1992, In: W. J. Duschl, S. J. Wagner, eds., Physics of Active Galactic Nuclei, Springer Heidelberg, p.484